Journal Pre-proof

Correlation of drilling cores and the Paks brickyard key section at the area of Paks, Hungary

Ágnes Novothny, Gabriella Barta, Tamás Végh, Balázs Bradák, Gergely Surányi, Erzsébet Horváth

PII: S1040-6182(19)30748-7

DOI: https://doi.org/10.1016/j.quaint.2019.09.012

Reference: JQI 7978

To appear in: *Quaternary International*

Received Date: 28 November 2018

Revised Date: 27 June 2019

Accepted Date: 12 September 2019

Please cite this article as: Novothny, Á., Barta, G., Végh, T., Bradák, B., Surányi, G., Horváth, E., Correlation of drilling cores and the Paks brickyard key section at the area of Paks, Hungary, *Quaternary International*, https://doi.org/10.1016/j.quaint.2019.09.012.

This is a PDF file of an article that has undergone enhancements after acceptance, such as the addition of a cover page and metadata, and formatting for readability, but it is not yet the definitive version of record. This version will undergo additional copyediting, typesetting and review before it is published in its final form, but we are providing this version to give early visibility of the article. Please note that, during the production process, errors may be discovered which could affect the content, and all legal disclaimers that apply to the journal pertain.

© 2019 Published by Elsevier Ltd.

Journal Pre-proof

Correlation of drilling cores and the Paks brickyard key section at the area of Paks, Hungary

Ágnes Novothny[1]*, Gabriella Barta[1], Tamás Végh[1], Balázs Bradák[1,2], Gergely Surányi[3], Erzsébet Horváth[1]

1. Eötvös Loránd University, Institute of Geography and Earth Sciences, Department of Physical Geography, Pázmány Péter sétány 1/C, Budapest, Hungary, H-1117
2. Department of Physics, University of Burgos, Av. de Cantabria, s/n 09006, Burgos, Spain
3. MTA-ELTE Geological, Geophysical and Space Sciences Research Group, Hungarian Academy of Sciences at Eötvös University, Pázmány Péter sétány 1/C. Budapest, Hungary, H-1117

* Corresponding author: novothnyagi@caesar.elte.hu
Keywords: loess, borehole, magnetic susceptibility, luminescence dating, Carpathian Basin

Abstract

The stratotype section of Paks brickyard provides the most detailed accessible loess-paleosol sequence from almost the entire Pleistocene in the middle part of the Carpathian Basin. The best and thickest loess archives of Hungary (Paks, Udvari-2A borehole) are preserved in this part of the basin and now two more drilling cores were deepened in this area on plateau position on loessic ridges: PA-I (~85 m) and PA-II (~50 m).

In absence of numerical dating method available for the entire records an attempt was made to compare the cores and correlate them to Marine Isotope Stages (MIS) mainly based on the variations of their MS curves and soil characteristics. Characteristic patterns of MS seem to help the identification of Marine Isotope Stages and therefore the correlation among the sections. Macroscopic investigation of the paleosols can support the correlation, although the coeval paleosols can have different appearances due to their different environmental conditions and topographic positions. Thirteen samples were dated using luminescence from the upper part of the cores, covering the age range of 20-200 ka to check and revise the supposed correlation. The MS based correlation supported by soil characteristics was only partly confirmed by luminescence data. Therefore, we emphasize that any correlation solely based on MS data or soil morphology, without any numerical age control, has to be taken with great caution. The different thickness and the present altitude of the coeval loess and paleosols imply differences and changes in paleogeomorphological positions of the investigated profiles during the Pleistocene. Significant subsidence and/or tectonic movements are the main causes of the deficient appearance of MIS 6-3 sediments in the Paks brickyard outcrop compared to the more complete sequences of the cores.

Journal Pre-proof

1. Introduction

The loess in the Carpathian Basin belongs to the center part of the loess belt in Europe. This basin, enclosed by high mountain chains (Fig. 1a), preserved sediments in large thickness from the Miocene to the Pleistocene, therefore provides great opportunity to study the Quaternary climate and environmental changes. The thickest and most complete loess-paleosol records in the Carpathian Basin – Mošorin-Stari Slankamen (Marković et al., 2011), Paks, Udvari 2A borehole (Koloszár, 2010; Sümegi et al., 2018) – retained sediments from late Early to Late Pleistocene. The Paks brickyard outcrop was the foremost and up to now the most investigated profile in Hungary. Although the investigation of the profile started at the end of the 19th century, it got into the centre of the interest in the middle of the 20th century (Ádám et al., 1954; Stefanovits et al., 1954; Kriván, 1955; Pécsi 1965). The outcrop has a thickness of 45 m above the base of the brickyard, but Ádám et al. (1954), Stefanovits et al. (1954), Kriván (1955) and Hahn (1977) drilled shallow (<15 m) boreholes along the loess wall to explore the lowest and oldest loess at the base of the sequence (Fig. 2). The Paks outcrop itself was investigated in numerous, different sections during the past decades. It is complicated to reconstruct the exact locations of these sections, since the walls retreated due to active mining processes. The original sections were excavated to various depth, provided different successions and therefore resulted in diverse interpretations. By these means and due to paleotopographic characteristics, the different descriptions sometimes lack the presence of certain paleosols (and/or other horizons) (Fig. 2). These differences highlight the fact that boreholes provide only point-wise information and possible hiatuses cannot be ruled out.

Fig. 1. Map of the Carpathian Basin (a) and land cover of the surrounding area of Paks (b). Red rectangle marks the position of the study area. DEM showing the topography of the study area (c). Location of the Paks brickyard outcrop and the boreholes (PA-I and II) are marked on this map.

The loess-paleosol record at the Paks brickyard outcrop can be considered as a relatively complete, quasi-continuous succession, which contains all paleosols used in the Hungarian loess stratigraphy. The loess-paleosol succession can be divided into two main units, as the 'Young Loess Series' and the 'Old Loess Series', as following the determination of Pécsi (1975). The classification of paleosols was made in numerous ways in the Hungarian Quaternary studies, which is summarized in Horváth and Bradák (2014). The application of the conventional soil classification system causes some difficulties, since post-burial processes may cause relevant alterations in paleosols. Therefore, the nomenclature by Pécsi (1993), similarly as it was summarized by Újvári et al. (2014), was applied during the description of stratigraphic units in our study, because it helps an easier follow-up especially with former publications (Fig. 2):

Journal Pre-proof

Journal Pre-proof

i) The ‘Old Loess Series’ has a thickness of almost 25 m at the Paks profile. Three reddish clay layers represent transition towards the Pliocene lacustric (water-lain) sediments at the basis of the series. The ‘Old Loess Series’ consists of mainly loess intercalated by the following paleosols, as from down to top:

a. Paks-Dunakömlőd paleosol (PDK) is a reddish-brown, Mediterranean-like soil with a characteristic $CaCO_3$ accumulation zone.

b. Paks Double pedocomplex (PD_1, PD_2) is composed of well-developed, reddish-brown to reddish Mediterranean-like soils, with strong $CaCO_3$ accumulation zones. The upper component is PD_1, which is thinner than the lower PD_2. PD_1 and PD_2 are divided by loess, which contains large carbonate concretions (diameters > 5-10 cm). Márton (1979) found the Brunhes-Matuyama paleomagnetic boundary (0.73 Ma) below PD_2, however later Pécsi et al. (1995) and Sartori et al. (1999) determined the BM boundary (0.78 Ma) from the upper part of PD_2.

c. Mtp_1 and Mtp_2 is a strongly developed clayey paleosol with hydromorphic features and of a possibly alluvial origin. The over- and underlying material also shows hydromorphic effects, especially iron and manganese features.

d. Phe is a weakly developed brown forest soil.

ii) The ‘Young Loess Series’ has a thickness about 25 m at Paks, which contains several thick paleosols, as from down to top:

a. Mende Base pedocomplex (MB) has two members: the upper one is MB_1, which is a thin Chernozem-like paleosol; the lower one is termed MB_2 and represents a brown forest soil, which is reddish-brown in colour. The basis of MB_2 is sandy loess, which shows signs of frost heaving (former segregational ice lenses).

b. Basaharc Lower paleosol (BA) is mostly identified as a forest steppe-like soil, but at the Paks and Basaharc sections it shows the characteristics of a strongly developed, brown forest soil (Horváth and Bradák 2014). In the loess between the BA and MB paleosols the Bag Tephra (BT) of canary yellow colour occurs (Pécsi 1985; Pécsi and Richter 1996). The BT is a marker horizon appearing in the loess successions of the Carpathian Basin. The high K-content suggests correlation with the Villa Senni Tuff in Italy (around 350 ka) (Horváth 2001).

c. Basaharc Double pedocomplex (BD) has two members divided by about 1m thick loess. The lower paleosol (BD_2) is a weakly developed forest steppe-like soil, whereas the upper one (BD_1) is well-developed. Characteristics of their development are clearly recognizable on magnetic susceptibility curves. BD pedocomplex can be correlated with MIS 7 (Horváth and Bradák 2014).

Journal Pre-proof

d. Mende Upper pedocomplex (MF) can be divided into two parts: the upper one (MF_1) is a weakly developed forest steppe-like soil, which has high charcoal content; the lower one (MF_2) is a well-developed brown forest soil. The formation of both paleosols happened unequivocally after MIS 6, based on dating results. Another tephra horizon called Paks Tephra (PT) can be found right above MF_1 paleosol, thus its age is around 30 ka based on the OSL data of the loess embedding the tephra layer. It has very similar heavy mineralogical composition to the Bag Tephra, therefore the same source area (Central Italy) can be assumed (Horváth 2001).

Fig. 2. Lateral variation of the loess-paleosol record at the Paks brickyard outcrop (based on Pécsi, 1984). Several different investigated profiles are indicated in the figure by the authors name and the year of their investigation. Vertical blue lines represent the locations of boreholes. Crescent-shaped features between BD and BA paleosols indicate delles with various infilling.

Since the beginning of the scientific investigation of the loess succession at the Paks brickyard almost all researchers made an attempt to correlate the loess-paleosol series with the glacial-interglacial cycles mainly based on the number of the paleosols. Kriván (1955) was the first who based his correlation on detailed sedimentological and paleontological results, since no absolute dating methods were available at that time. A decade later Pécsi (1965) used another assumption, that during an interglacial always forest soil development takes place. His assumption seemed to be supported by the results of the first radiocarbon and thermoluminescence (TL) datings (Pécsi 1975, 1993). As luminescence dating developed continuously, new chronostratigraphy of the Paks profile was published by Frechen et al. (1997) using infrared stimulated luminescence (IRSL) besides TL dating. Recently Thiel et al. (2014) confirmed this chronostratigraphy of the Paks profile with post-infrared infrared stimulated luminescence ($pIRIR_{290}$) dating. This practically means that each well-developed paleosol or pedocomplex in the stratigraphic column corresponds to the consecutive glacial cycle. Although the $pIRIR_{290}$ method has a much higher dating range, it is still limited to the upper third part of the Paks outcrop. Beneath this age limit one still must rely on sediment properties, like paleomagnetic orientation or magnetic susceptibility curves in order to seek the correlation of loess-paleosol series with MIS record. Beside chronostratigraphic investigations, other studies like geochemical (Újvári et al., 2014), magnetic properties, soil studies (Bradák et al. 2018a,b) were carried out at Paks brickyard outcrop, recently as well.

About 20 km W of the Paks brickyard the borehole Udvari 2A was drilled (Fig 1b, c). Based on magnetic polarity radiocarbon dating and MS curve of the borehole Koloszár (2010), Koloszár and Marsi (2010) and recently Sümegi et al., 2018 correlated the drilling with Marine Isotope Stages. The 97 m thick sequence also covers most probably the same time range as the Paks outcrop, therefore the borehole is considered as the thickest loess record from the Carpathian Basin.

Journal Pre-proof

The Paks brickyard outcrop (PBO) can be found on the right bank of the Danube, just right at the edge of the loess plateau (Fig. 1.). Several drillings were made in the adjacent area of Paks due to the exploration of industrial investments. Two boreholes were selected in this study as they are in the vicinity of the Paks outcrop and are composed of loess in large thickness. The PA-I drilling has been deepened in higher topographic position about 670 m N-NW from the brickyard, on the same loess ridge where the brickyard was formed. Compared to the brickyard, this area is in a more protected position in terms of morphology as it is farther from the edge of the loess plateau (Fig. 1b). The PA-II borehole is located in the inner part of the loess plateau, 6 km SW from the brickyard on the top of the next parallel loess ridge (Fig. 1b, c) in the highest topographic position. Apart from MS data, these boreholes are lack of numerical dating which would be necessary for the better correlation for this area. Aims of this study are i) to document and investigate these boreholes using luminescence dating and the carotage analysis (geophysical borehole logging: e.g. borehole diameter, natural gamma radiation, electrical resistance and in this study especially magnetic susceptibility curves); ii) to make a correlation between these boreholes and the Paks brickyard outcrop, (the now existing section wall, based on Thiel et al., 2014); and iii) to draw paleogeomorphological conclusions based on these comparisons.

2. Materials and methods

2.1 Boreholes and geophysical well logging

Boreholes were deepened into the surface using steel casing (with a diameter of 180/146 mm for PA-I and 250/219 or 219/165 mm for PA-II depending on the depth), thus the core was mostly undisturbed and light-tight material was available for investigation (sometimes the outer 2-3 cm of the cores were twisted, but the inner part was mainly intact). The boreholes and as well the geophysical logging were carried out by the Geo-Log Geophysical and Environmental Ltd. In the present study the magnetic susceptibility and the results of electrical resistivity logging were used from the dataset.

2.2 Stratigraphy of the cores

The stratigraphical description of both cores (PA-I and PA-II) can be found in Fig 3 a. Twenty-one and eighteen units were identified for the cores, respectively, based on field observations considering differences in colours, grain size distributions and pedogenic structures.

The PBO is a composite profile build-up of different bassets (Fig. 3b). The uppermost part, which expands down to the Bag Tephra (which is part of the overlying loess of the MB paleosol), is situated in the southern wall of the brickyard. The description is based on the work of Thiel et al., 2014 and Barta 2016 in this case. The lowermost part from below the BA paleosol was excavated in the northern wall, 100 m away from the western wall profile. The description of this part was made

Journal Pre-proof

Journal Pre-proof

after Pécsi et al. (1995).

Fig. 3. Simplified stratigraphic log of the drill-cores and the Paks brickyard outcrop with stratigraphical descriptions. a) PA-I and PA-II, b) PBO investigated by Pécsi et al. (1995) and the upper part of it investigated by Thiel et al. (2014) and Barta (2016).

2.3 Luminescence dating

2.3.1 Preparation of the samples, equipment

The time elapsed since the burial of the sediment can be dated by luminescence. As both quartz and feldspar minerals are abundant in loess, it is an ideal material for luminescence dating. Additionally, mineral dust has long transport distances, thus its previous luminescence signal is completely removed prior to deposition (Roberts, 2008).

The preparation of the samples was conducted under subdued red light. The polymineral fine grain fraction (4-11 μm) was extracted from the samples. All samples were treated using 0.1 N hydrochloric acid, 0.01 N sodium-oxalate and 30% hydrogen peroxide in order to remove carbonates, clay coatings and organic matter from the samples, respectively. The grains were mounted either on aluminium discs or stainless steel cups.

Luminescence measurements were performed using an automated Risø TL/OSL-DA-20 reader at the Institute of Geography and Earth Sciences at the Eötvös Loránd University. The reader is equipped with a bialkali EMI 9235QB photomultiplier tube, IR diodes (λ=875 nm), blue LEDs (λ=470 nm) and a ^{90}Sr /^{90}Y β-source irradiating the samples with a dose rate of ~0.07 Gy/s. A filter package of Schott BG-39 and BG-3, transmitting wavelengths between 350 and 420 nm, was placed in front of the photomultiplier in order to detect the blue light emission for IRSL measurements.

2.3.2 Equivalent dose determination

The Post-Infrared Infrared Stimulated Luminescence at 290°C ($pIRIR_{290}$) SAR (Single Aliquot Regeneration) protocol (Thiel et al., 2011) was applied for the measurements. This method is suitable for dating older materials, as the $pIRIR_{290}$ signal of feldspar saturates at higher doses, ~1000 Gy, which corresponds with ~250-330 ka in age considering a dose rate of 3-4 Gy/ka for loess. The other advantage of this method is, that the $pIRIR_{290}$ signal of feldspar shows less or even negligible fading (Thiel et al., 2011; Thomsen et al., 2011, Buylaert et al., 2009, 2012) therefore fading correction (Huntley and Lamoth 2001) is not necessary for age determination. This protocol includes an IR stimulation of 200 s at lower temperature (between 50 and 250°C), then an IR stimulation of 200 s at 290°C. The latter is used to measure the $pIRIR_{290}$ signal for the equivalent dose (D_e) determination. A preheat of 320°C for 60 s was applied prior to stimulations. At the end of each measurement cycle an IRSL stimulation at 325°C for 100 s was performed. The D_e values were obtained by integrating the first 4.4 s of the IRSL decay curve and the final 50 s of the

Journal Pre-proof

stimulation was subtracted to remove the background. A single or double saturating exponential function was fitted to the data points to assess the D_e of the aliquots.

A first IR stimulation temperature test was carried out on the lowermost and uppermost samples from core PA-I using test doses of ~140 Gy and ~42 Gy to test the D_e dependency on test dose size (Yi et al., 2016) and the first IR stimulation temperature (Buylaert et al., 2012, Yi et al., 2016). The first IR temperatures were increased with 50°C in each step between 50°C and 250°C. Figure 4 (a, b) shows the results of the test and demonstrates that there is only a slight effect of the different first IR stimulation temperatures and the test dose size on the D_e values for the younger sample. However, significant decrease of D_e is observed for both test dose size at higher first IR temperatures (200°C, 250°C) in case of the older sample.

Fading test was also carried out on the samples to assess how much the $pIRIR_{290}$ signals are affected by fading on different first IR stimulation temperature. The test was conducted on a young and an older sample using an artificial dose close to the natural D_e of the samples which was administered to the sample after bleaching. The delaying times were ranged between 0 and 60 hours. The $g_2$days fading rates were calculated for each aliquot. The results of the test clearly shows that the fading rate and therefore the signal stability is better applying higher first IR stimulation temperature (200°C) for both samples and for both test dose sizes (Fig. 4a,b). However, considering other samples from the cores which were involved to a general fading test applying $pIRIR_{290}$ at lower first IR temperature (50°C), the g-values are much better than for the previously tested samples (ranging between 0.16 and 1.93 %/decade with one outlier of -7.89%/decade) and a mean of 1.45±0.22 and 0.60±0.30 %/decade were calculated respectively for cores PA-I and PA-II. Below ~ 1.5 %/decade the fading rate is considered to be negligible (Thiel et al., 2011, Buylaert et al., 2012), therefore fading correction was not applied. The $pIRIR_{290}$ dose-response curve on Fig. 4c also do not shows significant fading for a saturated sample (PA-II 8). The first IR stimulation temperature was 50°C and the test dose was 140 Gy.

Dose recovery test was carried out on a relatively young sample to test whether the measurement sequence with different test dose sizes (~ 42 Gy and ~140 Gy) and first IR stimulation temperatures (50°C and 200°C) is successfully able to recover the previously administered dose, or not. To avoid the effect of poor bleach-ability of the natural $pIRIR_{290}$ signal the artificial beta dose (~105 Gy) was added on top of the natural dose (~115-130 Gy). Dose recovery ratio was calculated by subtracting the natural dose from the measured dose before dividing by the given dose. Fig. 4a shows the dose-recovery ratios using different settings. The best ratio (0.99±0.01) is yielded using 50°C for the first IR stimulation temperature and applying a test dose of ~140 Gy.

Some residual signal was observed after a 2-day daylight bleaching using the usual manner of $pIRIR_{290}$ SAR protocol with 50°C for the first IR temperature and 140 Gy as a test dose. The

Journal Pre-proof

observed residual signal increased with the burial age of the sample as it is shown in Fig. 4d Residual dose against D_e. Similar observations are reported by Buylaert et al. (2012) and Yi et al. (2016) and following the suggestion of Buylaert et al. (2012) the value of the interception of the fitted linear was subtracted as a residual from each the D_e-value for the age calculation.

Fig. 4. Luminescence test results: D_e as a function of the first IR stimulation temperature for sample PA-I 1 a), and PA-I 4 b). G_{2day}-values and dose-recovery results of the same samples are shown on the same plots with the 2nd Y-axis for them. Dose response curve of an aliquot of a saturated sample (PA-II 8) c). Residual dose of each sample is plotted against the $pIRIR_{290}$ D_e value for all samples.

Considering the results of all tests unless the fading results the basic settings of $pIRIR_{290}$ dating (using 50°C as the first IR stimulation temperature) with ~ 140 Gy test dose yielded the best results. Therefore, for final D_e measurements these settings were applied. The $pIRIR_{290}$ age estimate of a sample was calculated by taking the mean of the D_e-s of the five-ten measured aliquots. The $pIRIR_{290}$ signal of five samples (samples PA-I 5, 6 and PA-II 5, 6, 7) was beyond saturation (Murray et al., 2014), therefore only a minimum age could be calculated for these samples. Four-five samples yielded $pIRIR_{290}$ age from the cores which cover the upper third part of each core.

2.3.3 Dose rate determination

The surrounding sediment was collected from each luminescence position to determine the dose rate of the samples. The dose rates were obtained from the potassium, uranium and thorium content of the surrounding sediment, measured by gamma spectrometry in the laboratory at the Eötvös Loránd University, Institute of Geography and Earth Sciences (Table 1). An average a-value of 0.08±0.02 (Rees-Jones, 1995) was used for the calculation of feldspar IRSL. A potassium content of 12.5±1% (Huntley and Baril, 1997) was applied to calculate the dose rate for feldspar to account for the internal dose rate. The cosmic radiation was corrected for altitude and sediment thickness (Prescott and Hutton, 1994), assuming water contents of 15 or 20%, depending on the depth of the sample (20% was assumed if the depth of the sample was larger than 12 m). Dose rate conversion is based upon the factors of Gúerin et al. (2011). The dose rate of the lowermost samples of the cores were not measured and calculated as their burial age are far beyond the dating limit of $pIRIR_{290}$ method. We only assessed and average dose rate for these samples by calculating the mean of the dose rates from the corresponding cores.

*Table 1. Summary of the burial depths, radionuclide concentrations, dose rates, equivalent doses, and mean ages of $pIRIR_{290}$ dating on polymineral fine-grain samples. * dose rates are assumed as the average dose rate for the core.*

3. Results and discussion

3.1 Interpretation of magnetic susceptibility results

Journal Pre-proof

The first comparison of the PA-I and PA-II drilling cores with the Paks brickyard outcrop was carried out by applying the field description protocol and the results of the geophysical well logging provided by the Geo-Log Geophysical and Environmental Ltd. (magnetic susceptibility and resistivity logging). In European loess sequences, except some successions, paleosols are indicated by high magnetic susceptibility compare to their parent materials. Increasing magnetic susceptibility is the result of authigenic magnetic minerals e.g. formed by biogenic processes strongly connected to pedogenesis (Maher and Taylor, 1988; Evans, 2001). The application of pedogenic enhancement model in loess profile led to the generally accepted hypothesis about the relationship between higher magnetic susceptibility and the wetter and warmer 'soil forming' interglacial periods. Therefore, the patterns (shape and magnitude) of MS variations seem to help the identification of MI stages. Besides, based on these patterns of the MS curves the same paleosols might be identified in different loess-paleosol sections. Usually the shape and magnitude of the MS curve for the BD soils are characteristic, it has strong double peaks. The PD_1-PD_2-PDK paleosol-complex is characterised by three subsequent peaks with a two-fold peak uppermost, a three-fold peak in the middle and a weaker (smaller) peak at the bottom. These and other distinctive peaks were identified for both cores and matched with each-other and with the peaks of the PBO (Fig. 5). The correlation based on the MS patterns assumed some hiatuses (between 35 and 40 m for PA-II and above 10 m for PA-I), and the existence of an 'extra' soil for PA-I between 30 and 35 m (possible re-deposition and duplication of the previous one?). Summing up and considering the Hungarian nomenclature of the paleosols we supposed that MF is completely missing, but BA is present duplicated in PA-I, while either Mtp, or Phe is missing from PA-II (Fig. 5).

Figure 5. Correlation based on MS curves of the Paks brickyard outcrop (PBO) and the boreholes PA-I and II. Dashed lines refer to the first attempt of correlation, solely based on MS patterns. Question marks indicate those correlations, where no numerical dating was available.

3.2 Results of luminescence dating and their consequences for the stratigraphy

The oldest burial age for PA-I core (Fig. 6, Table 1) is 174±10 ka from Unit 5, right above the third well-developed paleosol. From below the soil only the minimum age could be determined. Therefore this thin paleosol is very likely equivalent with the BD paleosols, despite of its macroscopical features. However, it could not be determined whether this relatively thin paleosol is the BD_1, or the BD_2 or the superposition of both soils. The uppermost double paleosol was dated indirectly from the embedding loess (below, between and above the double soil). The $pIRIR_{290}$ ages of these samples resulted in ages of 145±8 ka for PA-I 3 from Unit 4, below the double paleosol, 86.5±5.9 ka for PA-I 2 from Unit 3, between the two paleosols and 28.2±1.6 ka from Unit 2, above the double paleosol. These ages indicate that the upper double paleosol is equivalent with MF_2 and MF_1 paleosols, which formed during MIS 5 and subsequently MIS 3, unlike our first impression and correlation, based on the MS pattern and soil characteristics of this pedocomplex (dashed lines on Fig. 5). This clearly shows, that chronostratigraphic interpretation based solely on the MS pattern and/or soil characteristics can be misleading. Numerical ages are crucial for the reliable correlation between sections or sections and MI stages (Stevens et al., 2018).

The two oldest $pIRIR_{290}$ ages from PA-II (Fig. 6) were determined from below the uppermost double paleosol complex. The ages (143±8 ka for PA-II 4 and 149±8 ka for PA-II 3, both samples from Unit 6) indicate that this loess was deposited during MIS 6, therefore the thick pedocomplex below this loess is very likely equivalent to the BD paleosol. This implication is supported by the fact that the sample below this pedocomplex (PA-II 5, lowermost part of Unit 7) resulted only in a minimum age, similar to the PA-I core. The uppermost double paleosol is equivalent to the MF_2 and MF_1 paleosols, as the $pIRIR_{290}$ age of the sample above these paleosols (PA-II 2, Unit 2) is 28.6±1.9 ka, indicating dust deposition during MIS 2. The youngest age from this core was determined from just below the modern soil (Unit 1) which yielded an age of 18.6±1.2 ka. This implies that modern soil developed in loess, which accumulated during MIS 2. The $pIRIR_{290}$ ages and our first correlation based on the MS were in agreement for the PA-II core (Fig. 5).

Comparing the $pIRIR_{290}$ ages of these cores to those of determined from the PBO by Thiel et al. (2014) we can conclude that the material in the uppermost part of the PBO profile and in the cores was deposited during MIS 3-2. The MF paleosols were only recognised in the cores but missing from that part of the PBO. Loess accumulated during MIS 6 was found in both cores and the outcrop as well. The $pIRIR_{290}$ ages determined from MIS 6 loess seems to be accurate, while Thiel et al. (2014) reported age overestimation from this part of the outcrop, possibly due to post-depositional mixing by crotovinas. From the cores only minimum ages were determined for the loess below the BD paleosol, while the corresponding sample from the PBO was still within the dating limit of $pIRIR_{290}$ method.

*Figure 6. PIRIR*290 *ages of PA-I and PA-II cores measured in this study and those of the PBO determined by Thiel et al., 2014. Cross-marks show the positions of the luminescence samples.*

3.3 Comparison of the PBO to the PA-I and PA-II cores – paleogeomorphological significance

The position of the boreholes and the brickyard outcrop are compared to each other on cross-sections (Fig. 7.), which derived from a digital elevation model (DEM) and were adjusted to the height above sea level. Fig. 7 shows that both cores and the brickyard outcrop are in a plateau position: PA-I is in an inner part of a loess ridge, further from the river Danube, in a geomorphologically protected location (less exposed to erosion), while PBO is on the edge of this ridge, close to the river (more exposed to erosion). PA-II is located in an inner part of an other loess ridge. The most secure and unequivocal connection could be made between PA-I and the PBO, because of the shortest distance of the locations.

Journal Pre-proof

Figure 7. Cross-section and stratigraphic log of the profiles through the area of Paks. Location of the Paks brickyard outcrop and the boreholes (PA-I and II) are marked.

The PA-I core contains in its 85 m thickness all the paleosols (Fig. 8) which are present in the 45-50 m thick sequence of the PBO. The MB – BA – BD paleosols are in almost similar height above sea level in PA-I and PBO, but all units below the MB paleosol were formed in deeper geomorphological position in PA-I in comparison to the corresponding layers in the PBO (Fig. 8). The assumed lower geomorphological position is also confirmed by the larger thickness and higher degree of development of the loess units and paleosols. The deeper geomorphological position could possibly be ceased gradually with the filling up of the depression. The compensation of the surface between PA-I and PBO ended with the pedogenesis of the Mende Base paleosol during MIS 11 and parallel depositional environment is supposed for the subsequent glacial periods until MIS 7. The reason of the filling up could be connected mainly to a higher rate of sediment accumulation, which happened through aeolian transport (loess formation), and probably by sheet wash, mass movements or the combination of these processes. The depression was possibly present before the beginning of the deposition of these layers, probably formed during the beginning of the Early Pleistocene. By the end of the Pleistocene a relief inversion can be observed between the areas of the PA-I core and the PBO. The uppermost third part of the loess record preserved in PA-I has three times larger thickness than that preserved in PBO. The Basaharc Double paleosol is the only unit in the entire sequence which is less developed in PA-I compared to PBO. Especially the loess deposited on the BD paleosols and the MF paleosols are preserved in bigger thickness in PA-I. The period between MIS 6 and 3 is scarcely represented in the PBO, in some parts it is preserved in ~ 1-2 m thickness (see in Pécsi et al. 1995), but in some parts it is completely missing (see in Thiel et al., 2014). The loess deposited during MIS 3-2 has again almost similar thickness (~ 10 m) in both sequences. The inequality in sedimentation during MIS 6-3 can be explained by i) considering higher sedimentation rate in the vicinity of PA-I core and/or less significant deflation due to its more protected plateau position, while the environment of PBO was probably closer to a wind channel between the two loess ridges in slope position (Fig. 1 c); ii) there was significant erosion, which translocated the greater part of MIS 6 – MIS 3 deposits (signs of slope wash or mass movement processes are frequent in this part of the outcrop); iii) the combination of the previously mentioned two processes. The reasons for intense erosion could be connected to local reasons, otherwise it must have affected the adjacent areas (around PA-I), as well.

- Theoretically, the sinking of the foreground of the loess plateau might give explanation for the recent plateau edge position of the brickyard outcrop and the tendency for erosion. The reason of the sinking is a dynamic subsidence at the western marginal part of the Great Hungarian Plain (along the actual course of the river Danube, South of Budapest) which

Journal Pre-proof

caused the Palaeo-Danube to gradually shift westwards from the axis of its previous alluvial fan and occupied its present course at the end of the Pleistocene. The timing of the shift is evidenced by the presence of the youngest (Late Weichselian or TII/a) terrace along the present Danube Valley in the Great Hungarian Plain (Pécsi 1959, Gábris et al. 2012). The shifting of the course of the river Danube caused the cut off of the steep Eastern edge of the loess ridges. This high bank has an elevation of >35 m higher than the floodplain of the Danube. However, between the recent course of the river Danube and the high bank there is a 3-4 km wide flood free terrace surface, and the high and low floodplains of the Danube in both directions, South and North, from Paks. The only exception is the area of PBO, where the river Danube directly flows in front of the high bank. This might imply that the subsidence is probably ceased or slowed down in almost all parts of the Western margin of the Great Hungarian Plain, but the area of PBO, where the subsidence could be more significant or long lasting. This might have caused the significantly less loess preservation of the PBO from the MIS 6-3 period and the erosional discordances of the PBO. However, recent study of Tóth et al. (2018) along the lower course of the Danube in the Great Hungarian Plain showed that major periods of subsidence could be dated around 20 ka and 7 ka. These results support the above mentioned (Ujházy et al., 2003; Gábris et al., 2012) results and make the above outlined theory questionable, as thick sediment succession was preserved from MIS 3-2 at the PBO.

- More probable reason, that the periodic intensifying activity of the local fault zone in Eastern direction from the edge of the loess plateau at Paks amplified the denudation of the plateau edge (based on geophysical investigations of Paks II. Zrt. Telephely engedélyezési dokumentáció. II. kötet/ 5. fejezet).
- During the Middle Pleistocene increasing tectonic activity in the Carpathian Basin and its surrounding were suggested by various studies. Geochemical investigations from the PBO (Újvári et al., 2014) showed that enhanced physical erosion of the source areas due to tectonism caused increasing dust sedimentation for the last 0.4 Ma (equal to 'Young Loess Series'). Buggle et al. (2013) described some change in the characteristics of paleosols by the possible influence of tectonic activity and orogenesis during the early Middle Pleistocene in the Middle and Lower Danube Basin. These results may support the theory about the connection between tectonic activity and the observed denudation events.

Comparing the PA-II core to PA-I and PBO we can conclude that the lower 20-25 m thick part of the PA-II core and the PBO profile has similar loess and paleosol thicknesses, however, differences occur in the degree of development of paleosols. The high similarity presumes identical formation conditions in terms of geomorphology. The lower part of the PA-I core (~ 55 m) has

Journal Pre-proof

much larger thickness than that of the PA-II core (~ 27 m), but this difference is almost levelled off for the BA-BD paleosols. The loess-paleosol succession in PA-II preserved the sediment of the MIS 6 – MIS 3 period in large thickness (almost 10 m) similarly to PA-I. PA-II contains the Mende Upper 1-2 paleosols as well, but only in a weakly developed state. Those loesses, which are younger than 30 ka, have almost similar thickness in both cores (12 and 10 m). This indicates that during the last two glacial cycles the sedimentation environment in the area of the two cores were quite similar, both were in plateau position, where dust accumulation was dominant over deflation.

Figure 8. Correlation of the profiles (PBO, PA-I and PA-II) based on pIRIR$_{290}$ ages and MS curves. Coeval horizons are connected. Question marks indicate those connections where no numerical dating was available. Profiles are placed according to their elevation above sea level.

The core of Udvari-2A (Koloszár, 2010; Koloszár and Marsi, 2010; Sümegi et al., 2018) contains the loess-paleosol sequence until the Ps8/1-8/2 (~PDK) soil almost in the same thickness as the core of PA-I, though it is 30 km away from the study area. Although some of the loess units are thicker or thinner, but all together both cores preserved the same thickness of sediment and soils (80-85 m) during the last ~0.9 Ma. These best preserved loess-paleosol sequences imply that the average accumulation rate for the Carpathian Basin could be around 9.8 cm/ka for the last 0.9 Ma, with a slight difference for the Old Loess Series (between MIS 21- MIS 12): ~7.8 cm/ka and for the Young Loess Series (between MIS 11- MIS 2): 11.8 cm/ka.

4. Summary

The Paks brickyard key section is considered as one of the most complete loess-paleosol sequence, available in an outcrop in Hungary. Recently two drillings were carried out in the vicinity of the outcrop. The investigation of the boreholes provides a good opportunity to compare them with each other and with the brickyard key section. As a backbone of an unequivocal correlation of various successions, it is crucial to apply numerical dating methods, as luminescence dating, even though its limit is ~250-300 ka for Hungarian loesses. Due to the limitation of numerical dating methods and as a support of the lithostratigraphical correlation, data from geophysical well logging, such as magnetic susceptibility and resistivity logging, can also be a useful tool. Although our correlation, based on MS curves and the physical characteristics of paleosol, was only partly confirmed by luminescence data (Fig. 8).

Our main findings during the correlation of the key section and the cores can be summarized as follows:

Journal Pre-proof

- Correlation based only MS values and/or paleosol characteristics without any numerical age control can be misleading.
- The correlation revealed very thick loess sedimentation from the Early to Late Pleistocene, PA-I core is one of the thickest and most detailed in the Carpathian Basin.
- The uppermost units of the PBO differ from the sequence of the PA-I and PA-II cores, since it very likely contains hiatuses between MIS 6 and 3 (190 – 40 ka). This can be explained i) by intensified erosion (by water or mass movements) of the Eastern edge of the loess ridges caused by either the gradual shifting of the river Danube to Western direction due to significant subsidence of smaller sub-basins at the edge of the Great Hungarian Plain (although new and old dating results pointed out that this probably happened around 20 ka, which is not consistent with the hiatuses at PBO), ii) or we can assume large denudation event(s) during the period of MIS 6-3 which can be caused by tectonic movements (renewed activity of a longer, NE-SW fault zone and/or a joint, shorter, N-S strike fault), iii) additionally decreased sedimentation rate and/or significant denudation should also be considered for the vicinity of PBO due to its proximity to a wind channel.

Acknowledgements

This work was funded by the National Research, Development and Innovation Office (NRDIO) project K119366. Special thanks to the Mecsekérc Ltd. B. Bradák acknowledges the financial support of project BU235P18 (Junta de Castilla y Leon, Spain) and the European Regional Development Fund (ERD). We also would like to thank to the anonymous reviewers for their valuable work on the earlier version of the manuscript which improved it significantly.

References

Ádám, L., Marosi, S., Szilárd, J. 1954. A paksi löszfeltárás. Földrajzi Közlemények 78/3, 239-254. (in Hungarian)

Barta, G. 2016. Analysis of secondary carbonates from the young loess-paleosol sequences of the Carpathian Basin - especially regarding their paleoenvironmental role (PhD dissertation (in English)). ELTE TTK, Budapest. http://dx.doi.org/10.15476/ELTE.2016.044. (https://edit.elte.hu/xmlui/handle/10831/33462).

Bradák, B., Újvári, G., Seto, Y., Hyodo, M., Végh, T. 2018a. A conceptual magnetic fabric development model for the Paks loess in Hungary. Aeolian Research 30, 20-31.

Bradák, B., Seto, Y., Hyodo, M., Szeberényi, J. 2018b. Relevance of ultrafine grains in the magnetic fabric of paleosols. Geoderma 330, 125-135.

Buggle, B., Hambach, U., Kehl, M., Marković, S. B., Zöller, L., Glaser, B. 2013. The progressive evolution of a continental climate in southeast-central European lowlands during the Middle Pleistocene recorded in loess paleosol sequences. Geology 41, 771–774.

Buylaert, J.-P., Jain, M., Murray, A.S., Thomsen, K.J. & Jain, M. 2009. Testing the potential of an elevated temperature IRSL signal from K-feldspar. Radiation Measurement, 44, 560–565.

Buylaert J.-P., Jain, M., Murray, A.S., Thomsen, K.J., Thiel, C., Sohbati, R. 2012. A robust feldspar luminescence dating method for Middle and Late Pleistocene sediments. Boreas 41, 435-451.

Evans, M. E., 2001, Magnetoclimatology of aeolian sediments, Geophys. J. Int., 144, 495-497.

Frechen, M.A., Horváth, E., Gábris, Gy. 1997. Geochronology of middle and upper Pleistocene loess sections in Hungary. Quaternary Research 48, 291–312.

Gábris, Gy. and Nádor, A. 2007. Long-term fluvial archives in Hungary: response of the Danube and Tisza rivers to tectonic movements and climatic changes during the Quaternary: a review and new synthesis. Quaternary Science Reviews 26, 2758–2782.

Gábris, G., Horváth, E., Novothny, Á. and Ruszkiczay-Rüdiger, Zs. 2012. Fluvial and aeolian landscape evolution in Hungary – results of the last 20 years research. Netherlands J. Geosci., 91 (1–2): 111–128.

Geo-Log Geophysical and Environmental Ltd. http://www.geo-log.hu/

Guérin, G., Mercier, N., Adamiec, G. 2011. Dose-rate conversion factors: update. Ancient TL 29, Issue 1, 5-8.

Hahn, Gy. 1977. A magyarországi löszök litológiája, genetikája, geomorfológiai és kronológiai tagolása. Földrajzi Értesítő 26, 1-28. (in Hungarian)

Horváth, E. 2001. Marker horizons in the loesses of the Carpathian Basin. Quaternary International 76/77, 157–163.

Horváth, E. and Bradák, B. 2014. Sárga föld, lősz, lösz: short historical overview of loess research and lithostratigraphy in Hungary. Quaternary International 319, 1-10.

Huntley, D.J., Baril, M.R. 1997. The K content of the K-feldspars being measured in optical dating or in thermoluminescence dating. Ancient TL 15, 11–13.

Huntley, D.J. & Lamothe, M. 2001. Ubiquity of anomalous fading in K-feldspars, and the measurement and correction for it in optical dating. Canadian Journal of Earth Sciences 38, 1093–1106.

Koloszár, L. 2010. The thickest and most complete loess sequence in the Carpathian Basin: the borehole Udvari-2A. Central European Journal of Geosciences 2/2, 165-174.

Koloszár, L., and Marsi, I. 2010. A Kárpát-medence legvastagabb és legteljesebb löszrétegsora: az Udvari-2A fúrás szelvénye és kvarter rétegtani jelentősége. (*The thickest and most complete loess sequence in the Carpathian Basin: the section of the borehole Udvari-2A and its significance in the Quaternary stratigraphy.*) Földtani Közlöny, 140/3, 251-262.

Journal Pre-proof

Kriván, P. 1955. A középeurópai plisztocén éghajlati tagolódása és a paksi alapszelvény. Magyar Állami Földtani Intézet Évkönyve 43, 363-510. (in Hungarian)

Maher, B.A., Taylor, R.M., 1988. Formation of ultrafine-grained magnetite in soils, Nature, 336, 368–370.

Marković, S.B., Hambach, U., Stevens, T., Kukla, G.J., Heller, F., McCoy, W.D., Oches, E.A., Buggle, B., Zöller, L., 2011. The last million years recorded at the Stari Slankamen loess–palaeosol sequence: revised chronostratigraphy and long-term environmental trends. Quaternary Science Reviews 30, 1142–1154.

Márton, P., 1979. Paleomagnetism of the Paks brickyard exposures. Acta Geologica Academiae Scientiarum Hungaricae 22, 443-449.

Murray, A.S., Schmidt, E.D., Stevens, T., Buylaert, J.P., Marković, S.B., Tsukamoto, S., Frechen, M., 2014. Dating Middle Pleistocene loess from Stari Slankamen (Vojvodina, Serbia) — limitations imposed by the saturation behaviour of an elevated temperature IRSL signal. Catena 117, 34–42.

Paks II. Zrt. Telephely engedélyezési dokumentáció. II. kötet/ 5. fejezet http://www.paks2.hu/hu/Kozerdeku/KozerdekuDokumentumok/telephelyengedelyezes/telephely_engedelyezes/Lapok/default.aspx

Pécsi, M. 1959. Formation and geomorphology of the Danube Valley in Hungary. 346 p., Budapest (Akadémiai Kiadó) [in Hungarian with German summary].

Pécsi, M. 1965. Upper Pleistocene paleogeography and the genetic study of the Upper Pleistocene deposits; the stratigraphic zoning of the loess profiles of the Carpathian Basin. Természetföldrajzi dokumentáció, INQUA SubKomission für Löss Stratigraphie Konferenz, Budapest, 1-16.

Pécsi, M. 1975. A magyarországi löszszelvények litosztratigráfiai tagolása. Földrajzi Közlemények 23, 217-230. (in Hungarian)

Pécsi, M. 1984. Is typical loess older than one million years? In: Pécsi, M. (ed.). Lithology and stratigraphy of loess and paleosols. INQUA Commissions on loess and paleopedology, Geographical Research Institute, Hungarian Academy of Science, 213-224.

Pécsi, M. 1985. Chronostratigraphy of Hungarian loesses and the underlying subaerial formation. In: Pécsi, M. (Ed.), Loess and the Quaternary – Chinese and Hungarian case studies. Akadémiai Kiadó, Budapest, 33-49.

Pécsi, M. 1993. Negyedkor és löszkutatás. Akadémiai Kiadó, Budapest, 375 p. (in Hungarian)

Pécsi, M., Schweitzer, F., Balogh, J., Balogh, M., Havas, J., Heller, F. 1995. A new loess-paleosol lithostratigraphical sequence at Paks (Hungary). Loess inForm 3, 63-78.

Pécsi, M. Richter, G. 1996. Loess: Origin – Classification – Landscape. Annals of Geomorphology

Journal Pre-proof

Journal Pre-proof

(in German with English summary). Gebrüder Brontraeger, Berlin, Stuttgart, 391 p.

Prescott, J.R., Hutton, J.T. 1994. Cosmic ray contribution to dose rates for luminescence and ESR dating: large depth and long-term time variations. Radiation Measurements 23, 497-500.

Rees-Jones, J. 1995. Optical dating of young sediments using fine-grain quartz. Ancient TL 13, 9-14.

Roberts, H. 2008. The development and application of luminescence dating to loess deposits: a perspective on the past, present and future. Boreas 37, 483–507.

Sartori, M., Heller, F., Forster, T., Borkovec, M., Hammann, J., Vincent, E. 1999. Magnetic properties of loess grain size fractions from the section at Paks (Hungary). Physics of the Earth and Planetary Interiors 116, 53-64.

Stefanovits, P., Kléh, Gy., Szüts, L. 1954. A paksi löszfal anyagának talajtani vizsgálata. Agrokémia és Talajtan. 1953. 4. sz.

Stevens, T., Buylaert, J.-P., Thiel, C., Újvári, G., Yi, S., Murray, A.S., Frechen, M., Lu, H. 2018. Ice-volume-forced erosion of the Chinese Loess Plateau global Quaternary stratotype site. Nature Communications. DOI: 10.1038/s41467-018-03329-2.

Sümegi, P., Gulyás, S., Molnár, D., Sümegi, B.P., Almond, P.C., Vandenberghe, J., Zhou, L., Pál-Molnár, E., Törőcsik, T., Hao, Q., Smalley, I., Molnár, M., Marsi, I. 2018. New chronology of the best developed loess/paleosol sequence of Hungary capturing the past 1.1 ma: Implications for correlation and proposed pan-Eurasian stratigraphic schemes. Quaternary Science Reviews 191, 144-166.

Thiel, C., Buylaert, J.-P., Murray, A., Terhorst, B., Hofer, I., Tsukamoto, S., Frechen, M. 2011. Luminescence dating of the Stratzing loess profile (Austria) - Testing the potential of an elevated temperature post-IR IRSL protocol. Quaternary International 234, 23-31.

Thiel, C., Horváth, E., Frechen, M. 2014. Revisiting the loess/palaeosol sequence in Paks, Hungary: A post-IR IRSL based chronology for the 'Younger Loess Series'. Quaternary International 319, 88-98.

Thomsen, K.J., Murray, A.S., Jain, M., 2011. Stability of IRSL signals from sedimentary K-feldspar samples. Geochronometria 38, 1-13.

Tóth, O., Sipos, Gy., Kiss, T., Bartyik, T., Filyó, D., Mezősi, G. 2018. Formation and age of floodplain surfaces along the Danube in Southern Hungary. Central European Conference on Geomorphology and Quaternary Sciences, Joint Conference of AKG and DEUQUA 2018. Book of Abstracts.

Ujházy, K., Gábris, Gy. and Frechen, M. 2003. Ages of periods of sand movement in Hungary determined through luminescence measurements. Quaternary International 111, 91–100.

Újvári, G., Varga, A., Raucsik, B., Kovács, J. 2014. The Paks loess-paleosol sequence: A record of

Journal Pre-proof

chemical weathering and provenance for the last 800 ka in the mid-Carpathian Basin. Quaternary International 319, 22-37.

Yi, S., Buylaert, J.-P., Murray, A. S., Lu, H., Thiel, C., Zeng, L. 2016. A detailed post-IR IRSL dating study of the Niuyangzigou loess site in northeastern China. Boreas 45, 644–657.

Figure captions

Figure 1. Map of the Carpathian Basin (a) and land cover of the surrounding area of Paks (b). Red rectangle marks the position of the study area. DEM showing the topography of the study area (c). Location of the Paks brickyard outcrop and the boreholes (PA-I and II) are marked on this map.

Figure 2. Lateral variation of the loess-paleosol record at the Paks brickyard outcrop (based on Pécsi, 1984). Several different investigated profiles are indicated in the figure by the authors name and the year of their investigation. Vertical blue lines represent the locations of boreholes. Crescent-shaped features between BD and BA paleosols indicate delles with various infilling.

Figure 3. Simplified stratigraphic log of the drill-cores and the Paks brickyard outcrop with stratigraphical descriptions. a) PA-I and PA-II, b) PBO investigated by Pécsi et al. (1995) and the upper part of it investigated by Thiel et al. (2014) and Barta (2016).

Figure 4. Luminescence test results: D_e as a function of the first IR stimulation temperature for sample PA-I 1 a), and PA-I 4 b). G_{2day}-values and dose-recovery results of the same samples are shown on the same plots with the 2nd Y-axis for them. Dose response curve of an aliquot of a saturated sample (PA-II 8) c). Residual dose of each sample is plotted against the $pIRIR_{290}$ D_e value for all samples.

Figure 5. Correlation based on MS curves of the Paks brickyard outcrop (PBO) and the boreholes PA-I and II. Dashed lines refer to the first attempt of correlation, solely based on MS patterns. Question marks indicate those correlations, where no numerical dating was available.

Figure 6. PIRIR290 ages of PA-I and PA-II cores measured in this study and those of the PBO determined by Thiel et al., 2014. Cross-marks show the positions of the luminescence samples.

Figure 7. Cross-section and stratigraphic log of the profiles through the area of Paks. Location of the Paks brickyard outcrop and the boreholes (PA-I and II) are marked.

Figure 8. Correlation of the profiles (PBO, PA-I and PA-II) based on $pIRIR_{290}$ ages and MS curves. Coeval horizons are connected. Question marks indicate those connections where no numerical dating was available. Profiles are placed according to their elevation above sea level.

Table caption

Table 1. Summary of the burial depths, radionuclide concentrations, dose rates, equivalent doses,

Journal Pre-proof

and mean ages of $pIRIR_{290}$ dating on polymineral fine-grain samples. * dose rates are assumed as the average dose rate for the core.

Journal Pre-proof

Sample ID	Depth (m)	Water cont. (%)	Th-232 [ppm]	U [ppm]	K [%]	Dose rate [Gy/ka]	pIRIR$_{290}$D$_e$ ± s.e. [Gy]	pIRIR$_{290}$age ± s.e. [ka]
PA-I 1	9.2	15 ± 5	12.10 ± 0.14	3.50 ± 0.03	1.61 ± 0.02	4.04 ± 0.21	114.1 ± 2.0	28.2 ± 1.6
PA-I 2	14.7	20 ± 5	11.13 ± 0.13	2.96 ± 0.02	1.25 ± 0.01	3.23 ± 0.18	279.8 ± 11.3	86.5 ± 5.9
PA-I 3	17.2	20 ± 5	10.44 ± 0.12	2.82 ± 0.02	1.39 ± 0.02	3.23 ± 0.17	469.1 ± 10.0	145 ± 8
PA-I 4	30.4	20 ± 5	13.25 ± 0.15	3.10 ± 0.02	1.71 ± 0.02	3.85 ± 0.20	669.1 ± 17.4	174 ± 10
PA-I 5	39.6					3.59 ± 1.79	> 1000	> 250-300
PA-I 6	43.8					3.59 ± 1.79	> 1000	> 250-300
PA-II 1	1.7	15 ± 5	9.37 ± 0.11	2.86 ± 0.02	1.07 ± 0.01	3.16 ± 0.18	58.7 ± 1.9	18.6 ± 1.2
PA-II 2	6.0	15 ± 5	10.52 ± 0.13	3.35 ± 0.03	1.25 ± 0.02	3.54 ± 0.20	81.4 ± 1.6	23.0 ± 1.4
PA-II 3	11.4	15 ± 5	11.52 ± 0.13	3.41 ± 0.02	1.40 ± 0.01	3.37 ± 0.18	96.2 ± 3.8	28.6 ± 1.9
PA-II 4	17.3	20 ± 5	10.95 ± 0.12	3.03 ± 0.02	1.44 ± 0.01	3.39 ± 0.18	505.2 ± 4.3	149 ± 8
PA-II 5	20.7	20 ± 5	12.34 ± 0.14	3.36 ± 0.02	1.69 ± 0.02	3.84 ± 0.20	549.7 ± 12.6	143 ± 8
PA-II 6	25.6					3.54 ± 1.58	> 1000	> 250-300
PA-II 7	32.5					3.54 ± 1.58	> 1000	> 250-300
PA-II 8	38.5					3.54 ± 1.58	> 1000	> 250-300

Journal Pre-proof

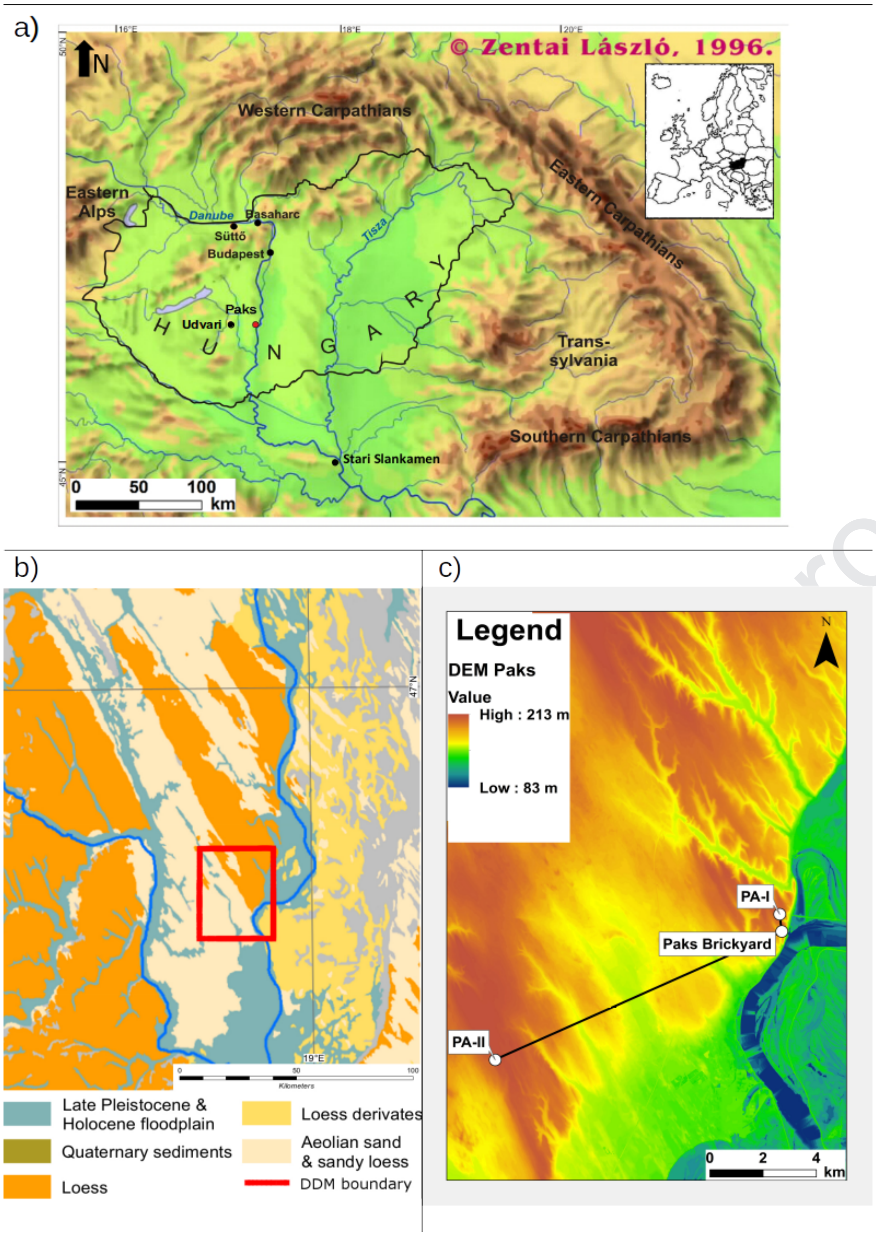
a)
N
© Zentai László, 1996.
Western Carpathians
Eastern Alps
Danube
Basaharc
Süttő
Budapest
Tisza
Eastern Carpathians
Paks
Udvari
H U N G A R Y
Trans-sylvania
Southern Carpathians
Stari Slankamen
0 50 100 km
b)
19°E
47°N
Kilometers
Late Pleistocene & Holocene floodplain
Quaternary sediments
Loess
Loess derivates
Aeolian sand & sandy loess
DDM boundary
c)
Legend
DEM Paks
Value
High : 213 m
Low : 83 m
N
PA-I
Paks Brickyard
PA-II
0 2 4 km

roof

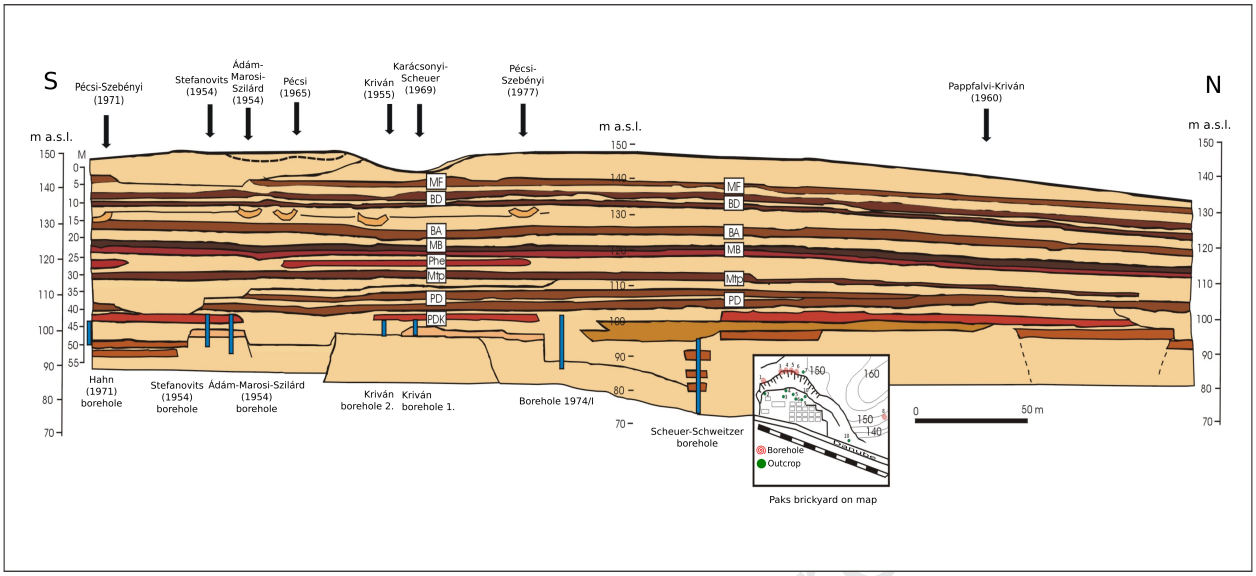

Journal Pre-proof

a)

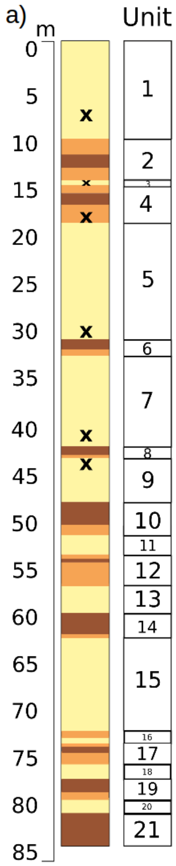

PA-I

1	0.35-9.50 m: greyish-yellow loess with mm-sized biogalleries. Redox features appearing scarcely.
2	9.50-14.40 m: dark brown paleosol (11.70-13.15 m) with its gradual upper (9.50-11.70 m) and lower (13.15-14.40 m) transition zones. Common presence of manganese nodules, hypocoatings, carbonate coatings and mm-sized carbonate concretions.
3	14.40-14.90 m: brownish-yellow loess, shows certain transitional habit between the Unit 2 and Unit 4 paleosols.
4	14.90-18.75 m: reddish-brown paleosol (15.70-16.90 m) with its upper (14.90-15.70 m) and lower (16.90-18.75 m) transition zones. The structure of the paleosol is homogenous, only its upper 40 cm is disturbed. Presence of secondary carbonates is only subordinated.
5	18.75-30.80 m: yellowish-grey sandy loess with sand intercalation between 20.00-23.50 m. Slight lamination between 27.70-28.80 m, possibly connected to former frost heaving processes.
6	30.80-32.50 m: brown paleosol with pinkish shade (30.80-31.90 m) and its lower transition (31.90-32.50 m).
7	32.50-41.90 m: greyish-yellow loess with weakly granular structure (sandy loess between 33.80-38.50 m). Presence of cm-sized biogalleries with reddish infilling in its lowermost 1.4 m.
8	41.90-43.25 m: reddish-brown paleosol (41.90-42.85 m) with cm-sized biogalleries and presence of hypocoatings. Lower transition zone (42.85-43.10 m) and $CaCO_3$ accumulation zone (43.10-43.25 m) are also present.
9	43.25-48.50 m: greyish-yellow loess/sandy loess with the presence of hypocoatings and calcified root cell structures.
10	48.50-51.50 m: reddish-brown paleosol (49.20-49.50 m) with its upper (44.45-49.20 m) and lower (49.50-51.50 m) transition zones. The upper transition is ochre yellow in colour, whereas the lower transition is yellowish brown. A thin carbonate bench is present between 50.40-50.50 m. Signs of former frost heaving processes are present as lamination between 50.50-51.30 m.
11	51.50-53.00 m: greyish-yellowish loess with higher fine sand component. Carbonate concretions appear in its lowermost 15 cm.
12	53.00-56.00 m: reddish-brown sandy paleosol (53.50-53.80 m) with the presence of hypocoatings, carbonate coatings. Carbonate concretions have reddish shade. Pebbles appear in its uppermost 10 cm. Presence of the upper (53.00-53.50 m) and lower (53.80-56.00 m) transition zones. Slight lamination between 54.20-54.60 m.
13	56.00-59.60 m: grey silt with fine sand component between 57.20-59.60 m.
14	59.60-62.00 m: brown paleosol with reddish patches (60.40-61.65 m), which is composed of clayey silt and is strongly cemented. Presence of its upper (59.60-60.40 m) and lower (61.65-62.00 m) transition zones.
15	62.00-72.30 m: greyish-yellow clayey material (62.00-66.70 m) with strong signs of hydromorphic processes (64.35-65.20 m), which changes to be greyish-yellow silt (66.70-72.30 m). Between 63.9 and 64.2 m high amount of large carbonate concretions can be found.
16	72.30-73.00 m: brownish loess (72.30-72.50 m), which changes to be yellowish loess (72.50-73.00 m).
17	73.00-75.60 m: reddish-brown paleosol with few ferruginous dots (73.45-74.00 m), with its upper transition zone (73.00-73.45 m) and $CaCO_3$ accumulation zone (74.00-75.60 m).
18	75.60-77.25 m: reddish-brown to greyish-yellow loess, with fine sand component between 75.60-76.60 m. Cm-sized biogalleries are present with reddish infilling.
19	77.25-79.00 m: reddish-brown paleosol (77.25-78.60 m) with fine sand component turning to be silty according to depth. Signs of strong bioturbation and soil structure is visible in krotovinas. Presence of $CaCO_3$ accumulation zone (78.60-79.00 m).
20	79.00-80.65 m: light reddish-brown silt with fine sand component (79.00-76.60 m), which seems to represent the lower part of a former paleosol. Presence of a $CaCO_3$ accumulation zone (79.60-79.95 m). Yellowish-reddish sand layer turning greyish-yellow with depth (79.95-80.65 m).
21	80.65-84.10 m: reddish-brown paleosol with sand component, with slight lamination between 81.70-81.80 m.

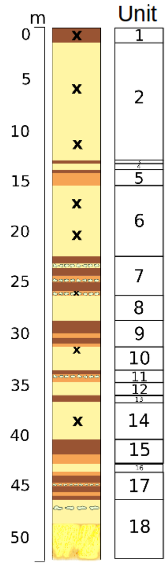

PA-II

1	0.0-1.50 m: dark brown modern soil, which gets lighter in colour with depth. Presence of hypocoatings and carbonate coatings.
2	1.50-13.10 m: yellowish-grey loess/sandy loess with hypocoatings.
3	13.10-13.40 m: brown paleosol with manganese dots, secondary carbonates (hypocoatings, carbonate coatings, calcified root cells) and charcoal. Krotovinas with loess infilling.
4	13.40-14.00 m: dominantly yellowish loess, which already shows the transitional characteristics with depth. Presence of krotovinas with soil infilling.
5	14.00-15.60 m: weakly developed light brown paleosol (14.00-14.30 m) with molluscs, secondary carbonates (hypocoatings, calcified root cells) and charcoal. Presence of its lower transition zone (14.30-15.60 m).
6	15.60-22.50 m: greyish-yellow loess with hypocoatings and carbonate coatings.
7	22.50-26.65 m: presence of multiple paleosol horizons. Brown paleosol (22.50-22.80 m) with its lower transition zone (22.80-23.40 m) and $CaCO_3$ accumulation zone (23.40-23.60 m). *Material is missing between 23.60-24.10 m due to drilling technique*. Light reddish-brown paleosol (24.10-24.40 m) with its strongly calcareous $CaCO_3$ accumulation zone (24.40-25.50 m). M*aterial is missing between 25.05-25.90 m due to drilling technique.* Presence of a $CaCO_3$ accumulation zone between 25.90-26.65 m.
8	26.65-28.80 m: greyish-yellow loess with manganese dots.
9	28.80-31.40 m: double paleosol. Pinkish brown paleosol (28.80-29.60 m), which gets a reddish shade according to depth. Presence of its $CaCO_3$ accumulation zone (30.10-30.50 m). Brown (slightly yellowish) paleosol (30.50-31.10 m) with secondary carbonates and its $CaCO_3$ accumulation zone (31.10-31.40 m).
10	31.40-33.70 m: greyish-yellow loess.
11	33.70-34.90 m: reddish-brown paleosol (33.70-34.10 m) with its $CaCO_3$ accumulation zone (34.10-34.90 m).
12	34.90-35.80 m: light brownish-yellow loess with molluscs.
13	35.80-36.00 m: light brownish-yellow loess, which contains multiple layers of carbonate concretions, which gives hints on the existence of a paleosol horizon.
14	36.00-40.50 m: light brownish-yellow loess with molluscs.
15	40.50-42.92 m: reddish-brown paleosol (40.70-41.30 m) with its lower transition zone (41.30-42.00 m) and $CaCO_3$ accumulation zone (42.00-42.92 m).
16	42.92-44.40 m: yellowish-brown loess.
17	44.40-47.40 m: multiple light reddish-brown paleosol horizons. Uppermost paleosol (44.40-45.00 m) with molluscs and its $CaCO_3$ accumulation zone (45.00-45.10 m). Middle paleosol (45.10-45.70 m) with its $CaCO_3$ accumulation zone (45.70-46.05 m). Lowermost paleosol (46.05-46.50 m) with its $CaCO_3$ accumulation zone (46.50-47.40 m).
18	47.40-52.50 m: yellowish brown fine sand (47.40-48.00 m) and reddish sand turning yellowish according to depth (48.00-52.50 m).

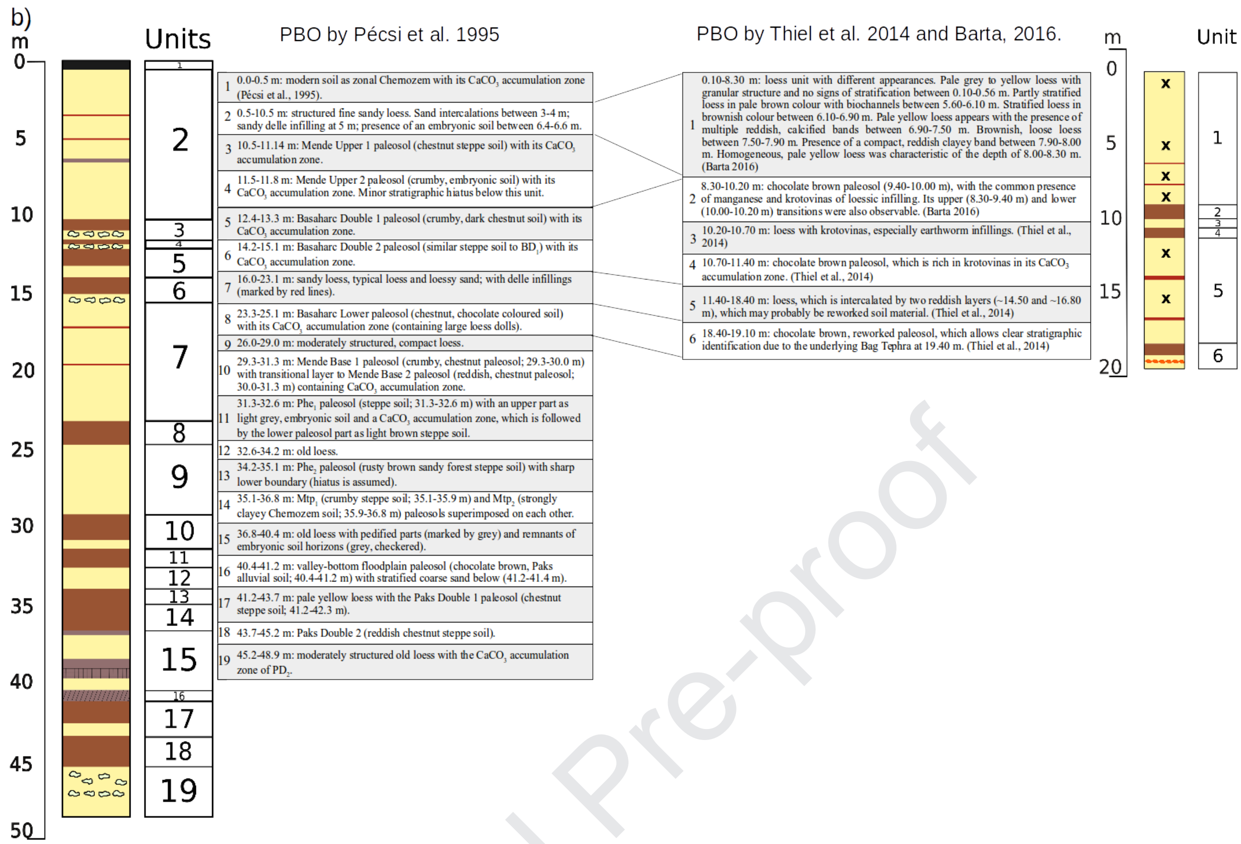

Journal Pre-proof

Journal Pre-proof

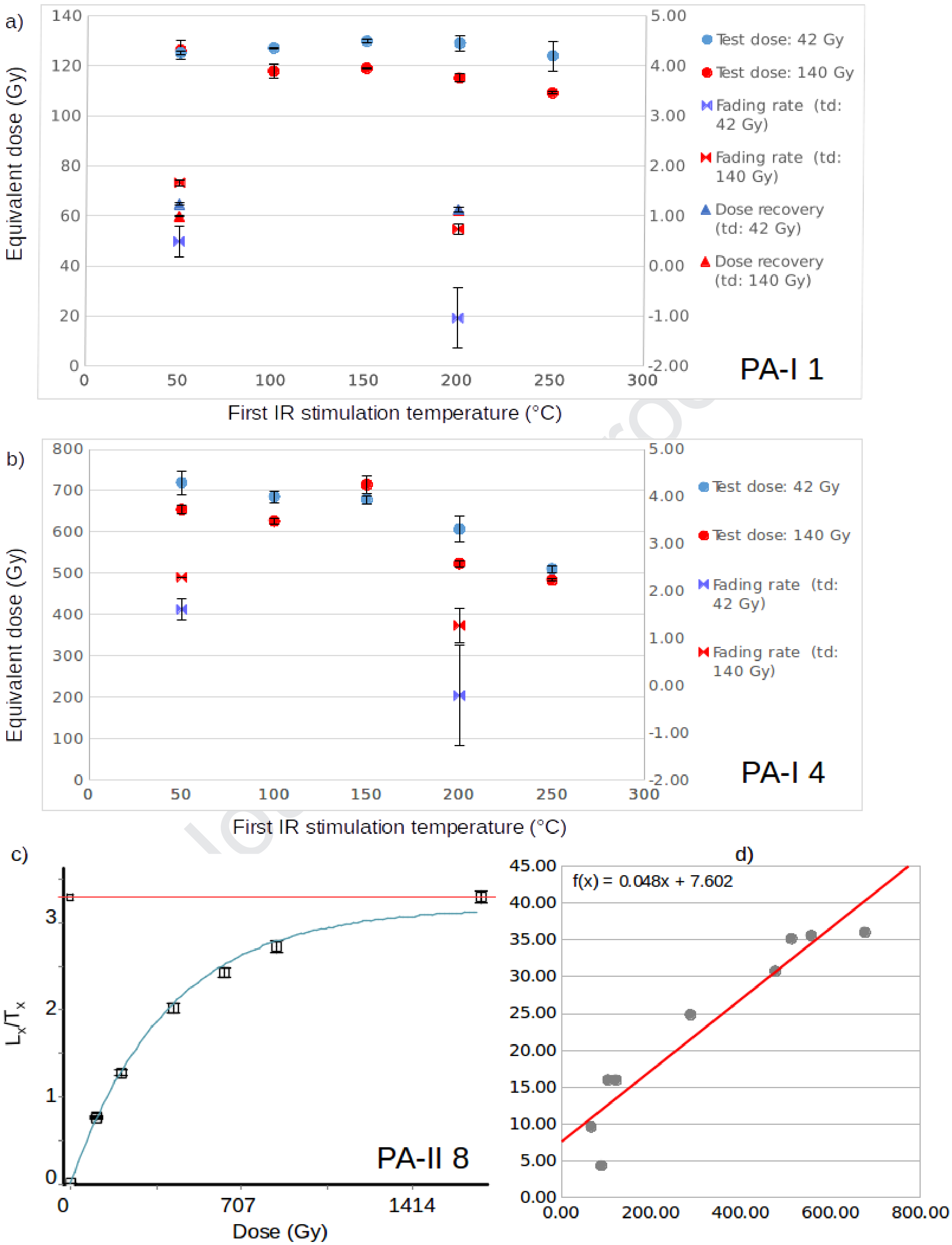

Journal Pre-proof

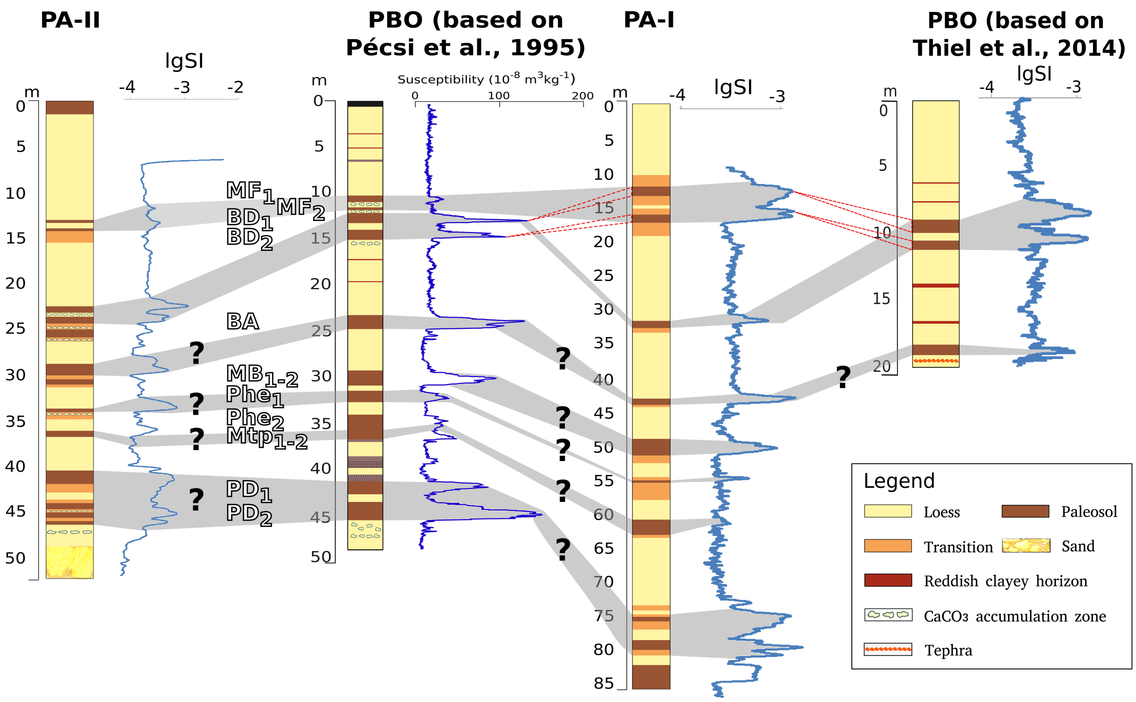

Journal Pre-proof

Journal Pre-proof

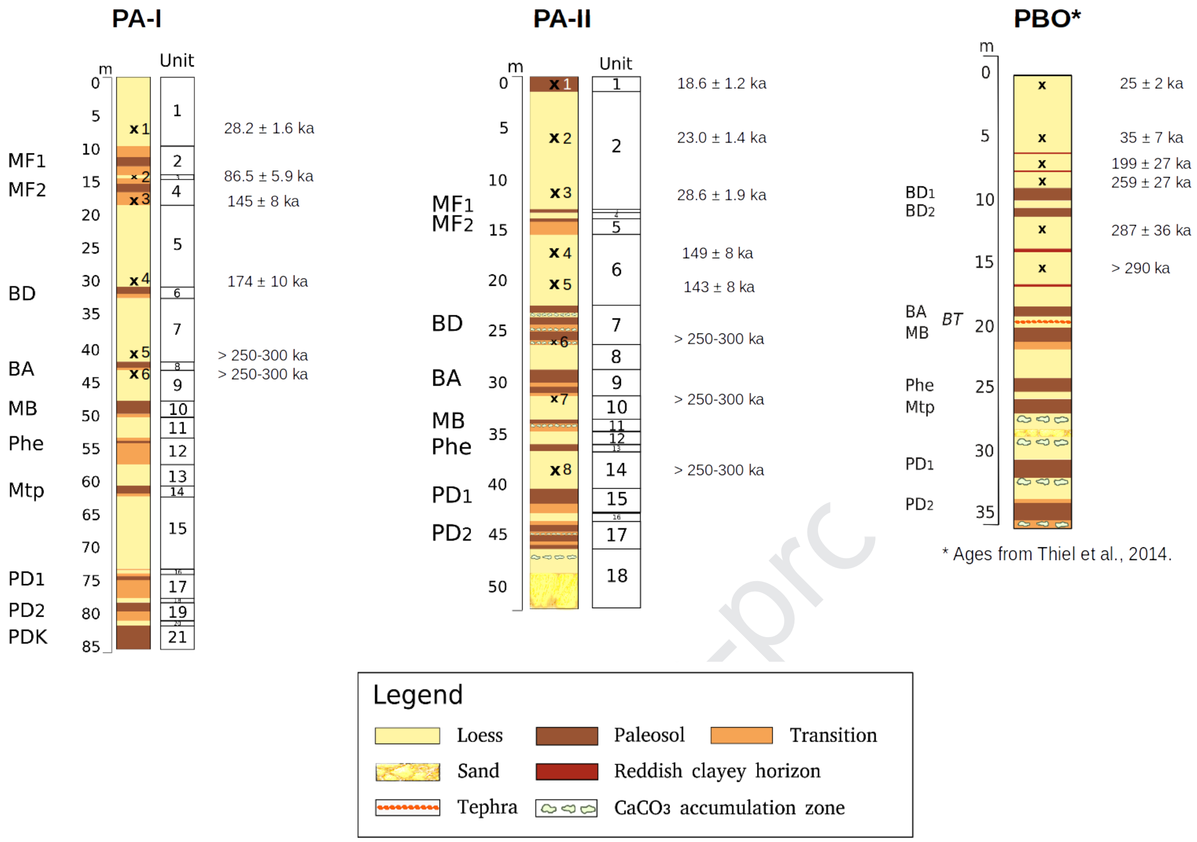

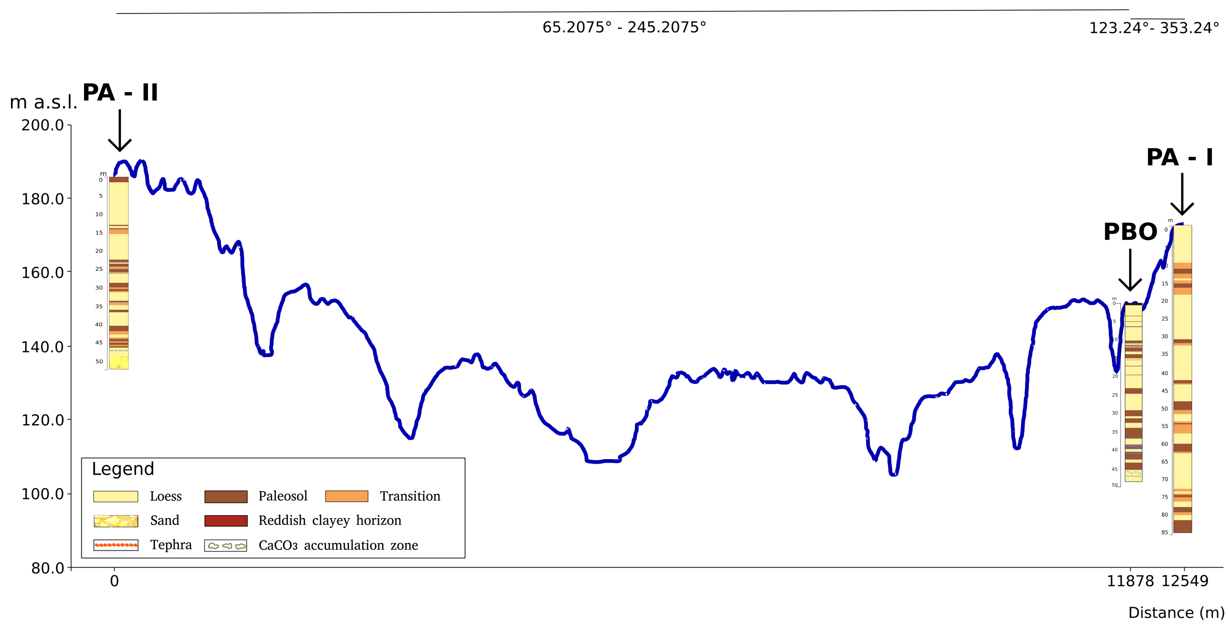

Journal Pre-proof

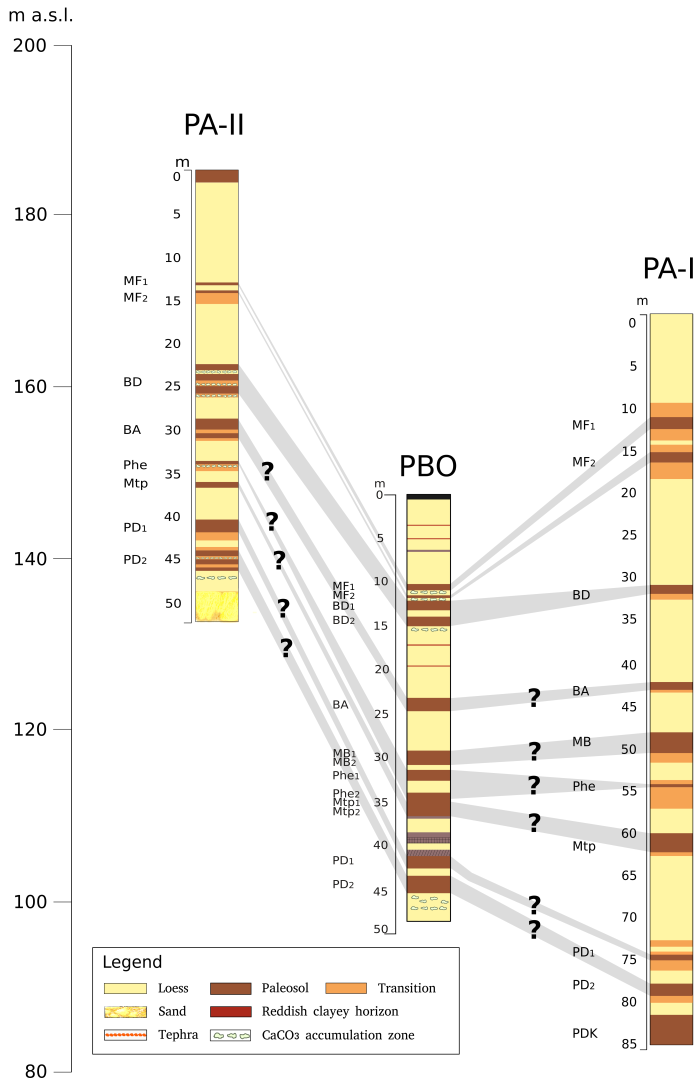
m a.s.l.
200
180
160
140
120
100
80
PA-II
PBO
PA-I
m
MF1
MF2
BD
BA
Phe
Mtp
PD1
PD2
MB1
MB2
Phe1
Phe2
Mtp1
Mtp2
BD1
BD2
MB
PDK
?
Legend
Loess
Paleosol
Transition
Sand
Reddish clayey horizon
Tephra
CaCO3 accumulation zone

proof